Journal of Biomolecular NMR, 5 (1995) 11–22
ESCOM

J-Bio NMR 266

Novel strategies for sensitivity enhancement in heteronuclear multidimensional NMR experiments employing pulsed field gradients*

M. Sattler**, M.G. Schwendinger***, J. Schleucher**** and C. Griesinger*****

Institut für Organische Chemie, Universität Frankfurt, Marie Curie Strasse 11, D-60439 Frankfurt, Germany

Received 13 October 1994
Accepted 11 January 1995

Keywords: B_0 gradients; COS-CT; COS-INEPT; In-phase COS-CT; Isotropic mixing; Multidimensional NMR; Planar TOCSY; HCCH-TOCSY; HNCO; Sensitivity enhancement

Summary

Novel strategies for sensitivity enhancement in heteronuclear multidimensional spectra are introduced and evaluated theoretically and experimentally. It is shown that in 3D sequences employing several **C**oherence **O**rder **S**elective **C**oherence **T**ransfer (COS-CT) steps, enhancement factors of up to 2 can be achieved. This sensitivity enhancement is compatible with the use of heteronuclear gradient echoes, yielding spectra with excellent water suppression. HNCO and HCCH-TOCSY pulse sequences are proposed and experimentally tested. These experiments employ recently developed coherence order selective pulse sequence elements, e.g., COS-INEPT and planar TOCSY for antiphase to in-phase transfers $2F^-S_z \leftrightarrow S^-$ or in-phase COS-CT for in-phase transfer $F^- \leftrightarrow S^-$, and the well-known isotropic TOCSY mixing sequences for homo- and heteronuclear in-phase transfer.

Introduction

Pulse sequences employing heteronuclear gradient echoes (Maudsley et al., 1978; Hurd and John, 1991) have been shown to yield spectra of very high quality with respect to artefact and solvent suppression, in combination with sensitivity enhancement (Palmer et al., 1991; Kay et al., 1992; Cavanagh and Rance, 1993; Schleucher et al., 1993a,b). Thus, for the structure determination of biomacromolecules it should be feasible to record all experiments on only one sample dissolved in H_2O, which is desirable with respect to the amount of sample needed and the comparability of the spectra. In experiments employing heteronuclear gradient echoes, either the echo ($S^+ \rightarrow I^-$) or the antiecho ($S^- \rightarrow I^-$) pathway of coherence orders is selected (in alternate scans), depending on the relative amplitude of the gradients used. However, employing a heteronuclear gradient echo in conventional experiments results in decreased sensitivity (Kay et al., 1992), unless mixing sequences are used that select either the echo or the antiecho pathway, even without employing a heteronuclear gradient echo (Schleucher et al., 1993a,b). For these **C**oherence **O**rder **S**elective **C**oherence **T**ransfers we introduce the name COS-CT. Several mixing sequences are known that provide COS-CT (Fig. 1).

The sensitivity-enhanced INEPT transfer which we henceforth call COS-INEPT (Fig. 1A) (Palmer et al., 1991; Kay et al., 1992; Cavanagh and Rance, 1993; Muhandiram et al., 1993; Schleucher et al., 1993a,b,1994; Muhandiram and Kay, 1994) and the heteronuclear planar TOCSY (Fig. 1B) (Schulte-Herbrüggen et al., 1991; Schleucher et al., 1994) achieve the transfer $2F_zS^- \rightarrow F^-$ in heteronuclear I_nS spin systems. These building blocks can therefore be used in conjunction with a heteronuclear gradient echo for the $X \rightarrow H$ transfer in HSQC-type experiments. In 2D experiments the use of these two mixing sequences for COS-CT, in combination with a heteronuclear gradient echo, provides an enhancement factor of $\sqrt{2}$ for IS spin systems compared to conventional experiments and a factor of 2 compared to con-

*This work has been presented in part at the 35th ENC, April 10–15, 1994, Asilomar, CA, U.S.A.
**Current address: Abbott Laboratories, 47G AP10, 100 Abbott Park Road, Abbott Park, IL 60064-3500, U.S.A.
***Current address: Department of Dermatology, University of Innsbruck, Anichstrasse 35, 6020 Innsbruck, Austria.
****Current address: Department of Biochemistry, University of Wisconsin-Madison, 420 Henry Mall, Madison, WI 53706, U.S.A.
*****To whom correspondence should be addressed.

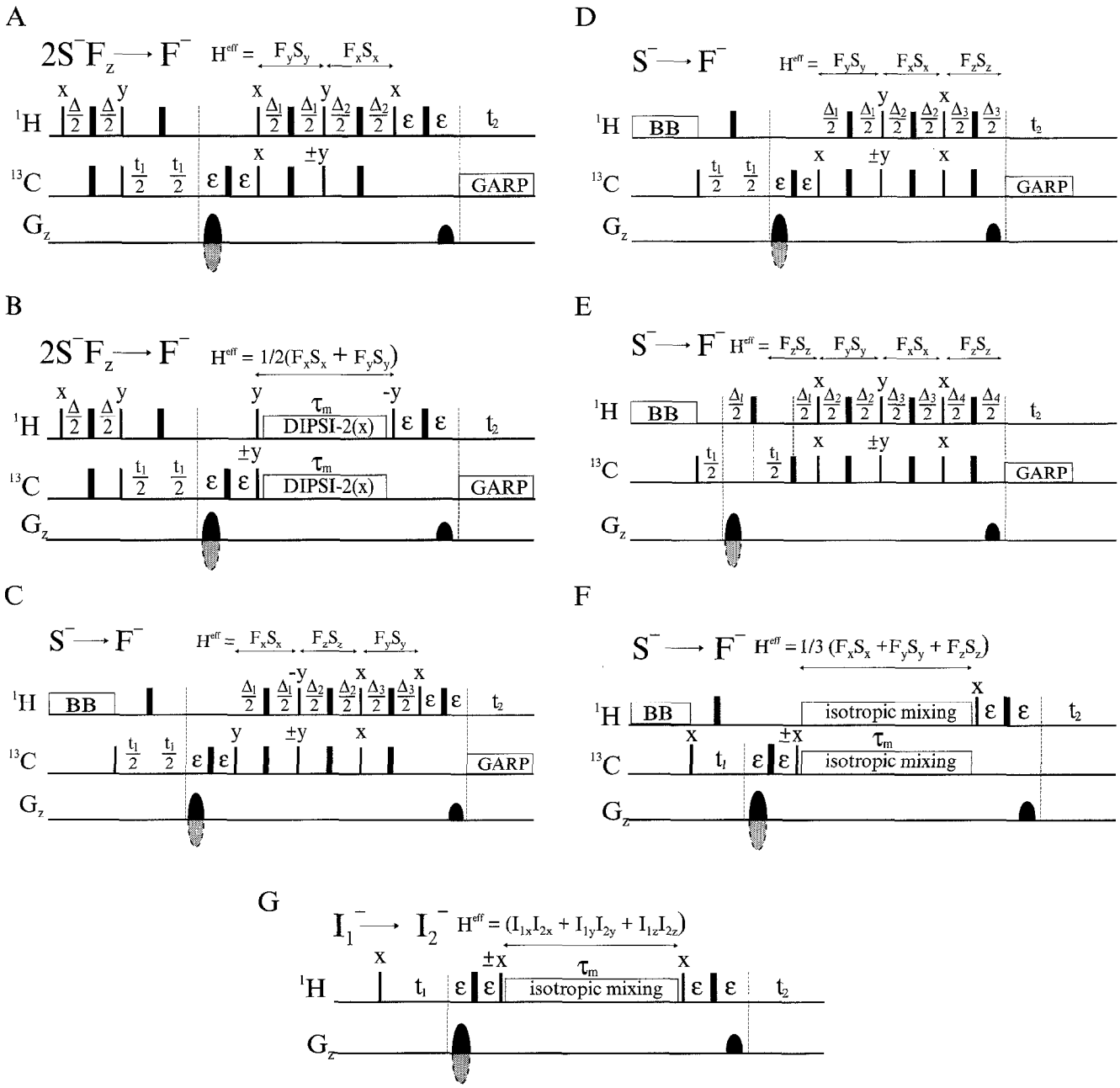

Fig. 1. COS-CT sequences. (A) COS-INEPT transfers antiphase coherence of the type $2F_zS^- \rightarrow F^-$. Whereas Δ_2 is set to $1/(2\,^1J(I,S))$, irrespective of the multiplicity, Δ_1 should be $0.3/^1J(I,S)$ for most uniform enhancement of all C-H multiplicities. (B) Planar heteronuclear TOCSY transfers antiphase coherence of the type $2F_zS^- \rightarrow F^-$. The mixing time τ_m should be set to approximately $0.77/^1J(I,S)$ for most uniform transfer for all multiplicities. (C) Sequence introduced by Vuister and Bax (1994) for the in-phase transfer $S^- \rightarrow F^-$. Most uniform excitation is achieved for $\Delta_1 = 0.27/^1J(I,S)$, $\Delta_2 = 0.35/^1J(I,S)$ and $\Delta_3 = 1/(2\,^1J(I,S))$. The sequence has the disadvantage that gradients cannot be applied during defocussing or refocussing of heteronuclear coupling constants. (D) Sequence introduced by Sattler et al. (1995) for the in-phase transfer $S^- \rightarrow F^-$. Most uniform excitation is achieved for $\Delta_1 = 0.31/^1J(I,S)$, $\Delta_2 = 0.23/^1J(I,S)$ and $\Delta_3 = 1/(2\,^1J(I,S))$. The sequence has the advantage that the proton gradient can be applied during refocussing of the heteronuclear coupling constants prior to acquisition. (E) Sequence introduced by Sattler et al. (1995) for the in-phase transfer $S^- \rightarrow I^-$ in an IS spin system, with $\Delta_1 + \Delta_4 = \Delta_2 = \Delta_3 = 1/(2\,^1J(I,S))$. The sequence has the advantage that both gradients can be placed in defocussing and refocussing periods of the heteronuclear coupling. (F) Heteronuclear isotropic mixing can be used for in-phase COS-CT $F^- \leftrightarrow S^-$. Optimal transfer times τ_m, disregarding homonuclear C,C couplings, are $3/(2\,^1J(I,S))$ for CH, $1/^1J(I,S)$ for CH_2 and $0.85/^1J(I,S)$ for CH_3 groups. A sequence is assumed that optimally transfers x- and z-magnetization. (G) Homonuclear TOCSY transfer via the isotropic J-coupling Hamilton operator. The implementation chosen to select either echo or anticcho works best with a TOCSY sequence that optimally transfers x- and z-magnetization, since x- and z-magnetization are prepared by the 90° pulses framing the homonuclear TOCSY.

ventional experiments with a heteronuclear gradient echo (Kay et al., 1992; Cavanagh and Rance, 1993; Muhandiram et al., 1993; Schleucher et al., 1993a,b; Muhandiram and Kay, 1994). For I_2S spin systems a factor of $\sqrt{2}$ is achieved compared to conventional experiments with a heteronuclear gradient echo and the feasibility of these

experiments has been demonstrated for all multiplicities (Schleucher et al., 1994).

Novel pulse techniques that achieve the in-phase heteronuclear transfer $S^- \leftrightarrow F^-$ have recently been introduced by Vuister and Bax (1994) (Fig. 1C) and Sattler et al. (1995) (Figs. 1D–F). For the heteronuclear in-phase transfer via COS-CT, an enhancement of $\sqrt{2}$ can be achieved for IS systems and $8/9\sqrt{2}$ for I_2S spin systems, with pulse sequences of acceptable duration and complexity. However, the efficiency for the $S^- \leftrightarrow F^-$ transfer is known to be below the theoretical maximum (Sattler et al., 1995; Stoustrup et al., 1995).

For COS-CT between homonuclear spins, the isotropic homonuclear coupling Hamiltonian is feasible (Braunschweiler and Ernst, 1983; Cavanagh and Rance, 1990) (Fig. 1G). A factor of $\sqrt{2}$ is achieved, irrespective of the spin system and without elongation of the mixing time.

Here we show that sensitivity enhancement can be achieved for each chemical shift evolution period in an n-dimensional NMR experiment, provided only COS-CT steps are used from the first evolution period to the detection period. Assuming a sensitivity enhancement per evolution period of $\sqrt{2}$, the sensitivity of an n-D experiment can therefore be improved by $2^{(n-1)/2}$. Thus, for 3D experiments a sensitivity enhancement of 2 can be achieved compared to conventional experiments without gradients.

Sensitivity of multidimensional NMR experiments employing COS-CT

Sensitivity enhancement via COS-CT in 2D NMR experiments

The COS-CT mixing sequences COS-INEPT and planar TOCSY achieve the following antiecho (A) transfer (Fig. 2A):

$$\text{A: } 2I_zS^- \rightarrow I^-e^{i\Omega_S t_1}e^{i\Omega_I t_2} \tag{1a}$$

and by incorporation of a 180°(S) pulse at an appropriate position, the corresponding echo (E) transfer is achieved:

$$\text{E: } 2I_zS^+ \rightarrow I^-e^{-i\Omega_S t_1}e^{i\Omega_I t_2} \tag{1b}$$

Hence, two FIDs are recorded that are modulated according to $e^{i\Omega_S t_1}e^{i\Omega_I t_2}$ and $e^{-i\Omega_S t_1}e^{i\Omega_I t_2}$. Complex Fourier transformation yields two peaks at ($\omega_1 = \Omega_S$, $\omega_2 = \Omega_I$) and ($\omega_1 = -\Omega_S$, $\omega_2 = \Omega_I$), each with signal intensity I = 1 (Fig. 3A). We assume that the standard deviation of the noise is $\sigma = 1$ at each peak position. Appropriate reflection at the $\omega_1 = 0$ axis to fold the two peaks on top of each other yields a signal of intensity 2 and noise of standard deviation $\sqrt{2}$. The signal-to-noise ratio is therefore $\sqrt{2}$. This is identical to the intensity of each individual signal I, namely I = 1, multiplied with the square root of the number of signals n at different positions in the spectrum (2 in this example) divided by the standard deviation of the noise σ (here 1):

$$S/N = I*\sqrt{n/\sigma} \tag{2}$$

In contrast, a conventional coherence transfer sequence effects the following transfers:

$$2I_zS_x \rightarrow I^- \cos(\Omega_S t_1)\, e^{i\Omega_I t_2} \tag{3a}$$

$$2I_zS_y \rightarrow I^- \sin(\Omega_S t_1)\, e^{i\Omega_I t_2} \tag{3b}$$

depending on the phase of the mixing sequence.

Complex Fourier transformation of these time domain signals yields four peaks at ($\omega_1 = \Omega_S$, $\omega_2 = \Omega_I$) and ($\omega_1 = -\Omega_S$, $\omega_2 = \Omega_I$), each with an intensity of I = 1/2 and noise of standard deviation $\sigma = 1$ (Fig. 3B). Appropriate reflections at the $\omega_1 = 0$ axis to fold the signals on top of each other yield a signal of intensity $S = 4 * 1/2 = 2$ and noise of standard deviation $\sigma = \sqrt{4} * 1 = 2$. The signal-to-noise ratio is therefore only S/N = 1. Again, the S/N ratio is identical

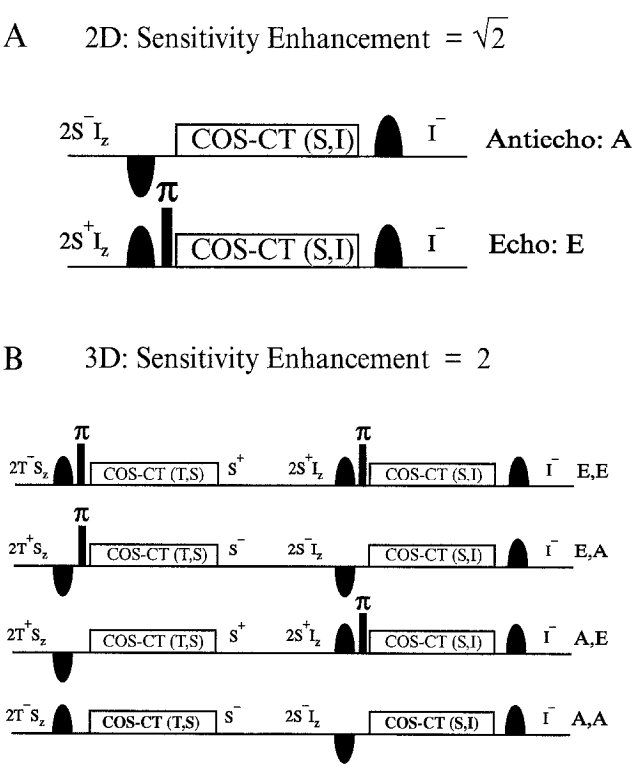

Fig. 2. (A) Schematic 2D sequence employing heteronuclear antiphase COS-CT. Two experiments that differ by the 180°(S) pulse and the sign of the gradient applied on the S spin are recorded, yielding the echo and the antiecho spectrum. (B) Schematic 3D sequence, employing COS-CT between t_1 and t_2 as well as between t_2 and t_3. Four different experiments with different gradient settings according to Eq. 3 have to be recorded, which yield the required echo and antiecho combinations in t_1 and t_2.

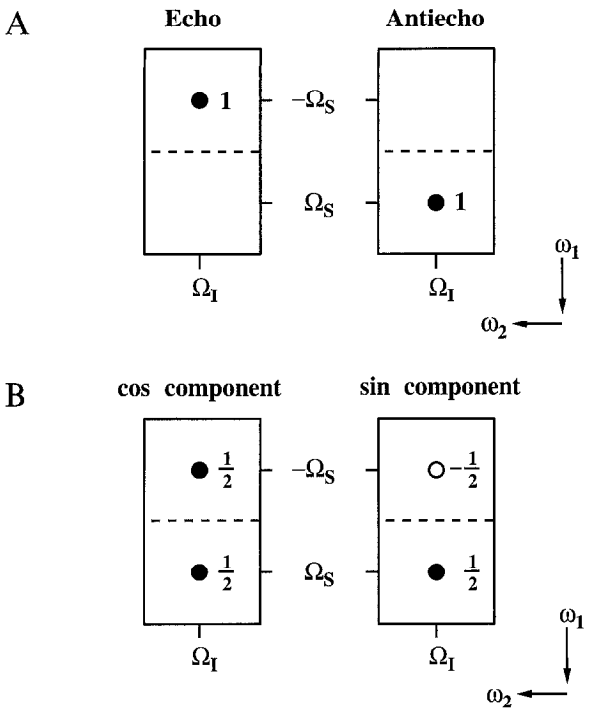

Fig. 3. (A) Echo and antiecho spectra obtained after complex Fourier transformation of the 2D FIDs obtained from Eq. 1. The signal is 1 and the noise is 1, too. Appropriate combination of the independent spectra yields an S/N of $\sqrt{2}$. (B) Cosine- and sine-modulated spectra obtained after complex Fourier transformation of the 2D FIDs obtained from Eq. 3. In the echo and antiecho parts, the signal is 1/2 and the noise is 1. Appropriate combination of the four peaks yields an S/N of 1.

to the intensity of each signal, I = 1/2, multiplied with the square root of the number of independent signals, 4, divided by the standard deviation of the noise ($\sigma = 1$).

From these considerations it can be deduced that enhancement is achieved only when COS-CT is performed between time periods during which chemical shift evolution takes place. When no chemical shift evolution of Ω_S takes place ($t_1 = 0$), the COS-CT yields a signal $e^{i\Omega_S t_1} e^{i\Omega_I t_2} = e^{i\Omega_I t_2}$. The conventional transfer, on the other hand, yields a signal $\cos(\Omega_S t_1)\, e^{i\Omega_I t_2} = e^{i\Omega_I t_2}$. Thus, no sensitivity enhancement is achieved. Nevertheless, COS-CT can be used to advantage even in this situation, if one wants to obtain the excellent water suppression achievable with heteronuclear echoes without loss of sensitivity compared to the conventional experiment, as will be shown below.

Concatenation of COS-CTs in multidimensional NMR experiments

To obtain the maximum sensitivity enhancement of 2 in a 3D experiment (Fig. 2B), at least two COS-CTs must be employed and the following four transfer pathways have to be recorded separately to obtain a 3D signal with pure phases (we consider a heteronuclear linear three-spin system, T-S-I, with evolution of chemical shifts Ω_T, Ω_S and Ω_I and appropriate couplings during t_1, t_2 and t_3, respectively):

$$
\begin{aligned}
\text{A/A:}\quad & 2S_zT^- \xrightarrow{\Omega_T} 2S_zT^- \rightarrow S^- \xrightarrow{\Omega_S} 2I_zS^- \\
& \rightarrow I^- \xrightarrow{\Omega_I} I^-\, e^{i\Omega_T t_1}\, e^{i\Omega_S t_2}\, e^{i\Omega_I t_3} \\
\text{E/A:}\quad & 2S_zT^+ \xrightarrow{\Omega_T} 2S_zT^+ \rightarrow S^- \xrightarrow{\Omega_S} 2I_zS^- \\
& \rightarrow I^- \xrightarrow{\Omega_I} I^-\, e^{-i\Omega_T t_1}\, e^{i\Omega_S t_2}\, e^{i\Omega_I t_3} \\
\text{E/E:}\quad & 2S_zT^- \xrightarrow{\Omega_T} 2S_zT^- \rightarrow S^+ \xrightarrow{\Omega_S} 2I_zS^+ \\
& \rightarrow I^- \xrightarrow{\Omega_I} I^-\, e^{i\Omega_T t_1}\, e^{-i\Omega_S t_2}\, e^{i\Omega_I t_3} \\
\text{A/E:}\quad & 2S_zT^+ \xrightarrow{\Omega_T} 2S_zT^+ \rightarrow S^+ \xrightarrow{\Omega_S} 2I_zS^+ \\
& \rightarrow I^- \xrightarrow{\Omega_I} I^-\, e^{-i\Omega_T t_1}\, e^{-i\Omega_S t_2}\, e^{i\Omega_I t_3}
\end{aligned}
\qquad (4a)
$$

Such sequences produce four signals with intensity 1. Therefore, Eq. 2 yields a signal-to-noise ratio of 2. In standard 3D experiments, the following four amplitude-modulated transients are recorded to obtain pure phases:

$$
\begin{aligned}
& 2S_zT_x \xrightarrow{\Omega_T} 2S_zT_x \rightarrow -S_y \xrightarrow{\Omega_S} 2I_zS_x \rightarrow I^- \\
& \xrightarrow{\Omega_I} I^- \cos(\Omega_T t_1) \cos(\Omega_S t_2)\, e^{i\Omega_I t_3} \\
& 2S_zT_x \xrightarrow{\Omega_T} 2S_zT_y \rightarrow -S_y \xrightarrow{\Omega_S} 2I_zS_x \rightarrow I^- \\
& \xrightarrow{\Omega_I} I^- \sin(\Omega_T t_1) \cos(\Omega_S t_2)\, e^{i\Omega_I t_3} \\
& 2S_zT_x \xrightarrow{\Omega_T} 2S_zT_x \rightarrow -S_y \xrightarrow{\Omega_S} 2I_zS_y \rightarrow I^- \\
& \xrightarrow{\Omega_I} I^- \cos(\Omega_T t_1) \sin(\Omega_S t_2)\, e^{i\Omega_I t_3} \\
& 2S_zT_x \xrightarrow{\Omega_T} 2S_zT_y \rightarrow -S_y \xrightarrow{\Omega_S} 2I_zS_y \rightarrow I^- \\
& \xrightarrow{\Omega_I} I^- \sin(\Omega_T t_1) \sin(\Omega_S t_2)\, e^{i\Omega_I t_3}
\end{aligned}
\qquad (4b)
$$

Since the number of signals is doubled for each evolution period compared to the COS-CT experiment (two signals occur at $\pm\,\Omega_T$ and $\pm\,\Omega_S$ in ω_1 and ω_2, respectively), a total number of n = 16 independent peaks of intensity I = 1/4 are obtained, yielding a signal-to-noise ratio of $S/N = (1/4)\sqrt{16} = 1$. Thus, an enhancement factor of $2^{(n-1)/2}$ can be achieved for an n-D experiment using exclusively COS-CTs between t_1 and the detection compared to a standard n-D experiment. However, this ratio cannot always be achieved, due to the fact that *heteronuclear* COS-CT requires more time than the conventional coherence transfer, as shall be explained below.

Time requirements for COS-CT

As noted above, sensitivity enhancement can only be obtained if all coherence transfers following the t_1 evolution period are also coherence order selective. This holds even for transfers between durations with no chemical shift evolution, since otherwise one of the magnetization components is lost, which leads to a reduction in S/N. Therefore, in order to decide from which evolution time on COS-CT should be used in a multidimensional experi-

ment, the time requirements for COS-CT compared to the conventional coherence transfers must be known. This shall be derived in the following.

Consider the transfer of heteronuclear antiphase coherence to in-phase coherence, i.e., $2I_zS^- \rightarrow I^-$ in an IS spin system. Fully selective transfer without generation of additional operators is possible, as has been shown by Palmer et al. (1991). In order to find the fastest transfer, the chemical shift is ignored since it does not interfere with the refocussing of antiphase coherence to in-phase coherence. The Hamiltonian must be invariant with respect to rotation about the z-axis, since the coherence order is to be conserved. Thus, the Hamiltonian must be a superposition of the following three terms: I_zS_z, $I_xS_x + I_yS_y$ and $I_xS_y - I_yS_x$. The term I_zS_z commutes with the two other Hamiltonians. In addition, it does not contribute to the transfer $2I_zS^- \rightarrow I^-$ and can therefore be neglected. $I_xS_x + I_yS_y$ and $I_xS_y - I_yS_x$ are identical, except for a trivial rotation by 90° about the S_z or I_z axis, which amounts to a phase for either the initial or the final coherence, $2I_zS^-$ or I^-. Therefore, we can focus on the $I_xS_x + I_yS_y$ term. This effective Hamiltonian can be formed from the weak coupling Hamiltonian $2\pi JI_zS_z$ by a multiple pulse sequence. Since any pulse sequence can be represented by unitary propagators, the general theorem for coherence transfer (Sørensen, 1989,1990,1991; Redfield, 1991; Levitt, 1992a,b; Nielsen and Sørensen, 1992) can be applied to find the maximum projection (a_{max}) of the weak coupling Hamiltonian $2\pi JI_zS_z$ ($\sigma_{diag}^{initial}$) onto the desired Hamiltonian of the form $I_xS_x + I_yS_y$ (σ_{diag}^{final}). This can be derived by analysis of the eigenvalues of the respective Hamiltonians. For $2\pi JI_zS_z$, we find the eigenvalues $\pi J/2$, $\pi J/2$, $-\pi J/2$ and $-\pi J/2$. For $I_xS_x + I_yS_y$, we find the eigenvalues 1/2, 0, 0 and −1/2. With the formula:

$$a_{max} = \frac{Tr(\sigma_{diag}^{initial}\,\sigma_{diag}^{final})}{Tr(\sigma_{diag}^{final}\,\sigma_{diag}^{final})} = \frac{2 * \pi J/4}{2 * 1/4} = \pi J \qquad (5)$$

it is obvious that the maximum weight with which $I_xS_x + I_yS_y$ can be formed from $2\pi JI_zS_z$ is πJ for any pulse sequence. This effective Hamiltonian must be active during a delay 1/J to achieve full transfer. Compared to transfer of one Cartesian component $2I_zS_x$ to I_y, which takes only 1/(2J) in a normal INEPT step, the time required is larger by a factor of 2. This is a general result and shows that the sequences found until now cannot be further improved with respect to transfer speed. Therefore, reduced enhancement is expected unless the reciprocal T_2 times of the spins involved are considerably smaller than the heteronuclear coupling employed for the COS-CT. Enhancement is therefore only achieved for:

$$\exp[-1/(2J_{IS}T_{2S})] \geq 1/\sqrt{2} \qquad (6)$$

Since the COS-CT sequences usually have more pulses, Shigemi tubes (Shigemi Inc., Allison Park) were used to minimize effects of B_1 inhomogeneity on sensitivity.

Experiments and Results

HNCO

The HNCO experiment is constructed from four coherence transfer steps. If we choose I for H^N, S for N and T for C', the following transfers are accomplished in the conventional HNCO sequence, which transfers one Cartesian magnetization component in each step (Fig. 4A):

$$\begin{aligned} &2I_yS_z \xrightarrow{\text{(a) } \pi/2_x(I,S)} 2I_zS_y \\ &2S_yT_z \xrightarrow{\text{(b) } \pi/2_x(S,T)} 2S_zT_y \xrightarrow{\text{(c) } \pi/2_x(S,T)} 2S_yT_z \\ &2I_zS_y \xrightarrow{\text{(d) } \pi/2_x(I,S)} 2I_yS_z \end{aligned} \qquad (7a)$$

In order to make the most efficient use of COS-CT, the chemical shift evolution of C' is performed before the chemical shift evolution of N and the two latter coherence transfers are replaced by COS-CTs (Fig. 4B):

$$\begin{aligned} &2I_yS_z \xrightarrow{\text{(a) } \pi/2_x(I,S)} 2I_zS_y \\ &2S_yT_z \xrightarrow{\text{(b) } \pi/2_x(S,T)} 2S_zT^- \xrightarrow{\text{(c) COS-CT(T,S)}} S^- \\ &2I_zS^- \xrightarrow{\text{(d) COS-CT(S,I)}} I^- \end{aligned} \qquad (7b)$$

In the last coherence transfer step of Eq. 7b, starting from S^- in-phase magnetization, heteronuclear antiphase coherence $2I_zS^-$ is obtained by defocussing during $1/(2J_{IS})$ and it is transferred by COS-CT: $S^- \rightarrow 2I_zS^- \rightarrow I^-$. This transfer $S^- \rightarrow I^-$ can also be considered as in-phase COS-CT. In I_nS spin systems with $n > 1$, the pulse sequences given in Figs. 1C–F achieve better transfers than the sequence given in Fig. 4B for the $S^- \rightarrow F^-$ in-phase COS-CT. Only for IS spin systems the sequences yield identical transfer efficiencies.

COS-CT provides another possibility, namely to use it only for the final $S \rightarrow I$ coherence transfer step (Fig. 4C). Then only a factor of $\sqrt{2}$ in S/N can be gained compared to the conventional HNCO experiment without heteronuclear gradient echo. This experiment was introduced by Schleucher et al. (1993) and discussed in great detail by Muhandiram and Kay (1994). Even when no ^{15}N spin evolution takes place before the final $^{15}N \rightarrow {}^1H$ transfer, like in a H(N)CO correlation which is, for example, part of a CBCACO(N)H experiment, the formation of a heteronuclear gradient echo is recommended because of the excellent water suppression to be achieved. Evolution of carbonyl chemical shifts instead of ^{15}N chemical shifts is advantageous when the $^{15}N,^1H$ shift correlation is less well resolved than the H(N)CO correlation. The sensitivity of this 'relayed' H(N)CO experiment, which corresponds to the pulse sequence of Fig. 4C without the ^{15}N chemical

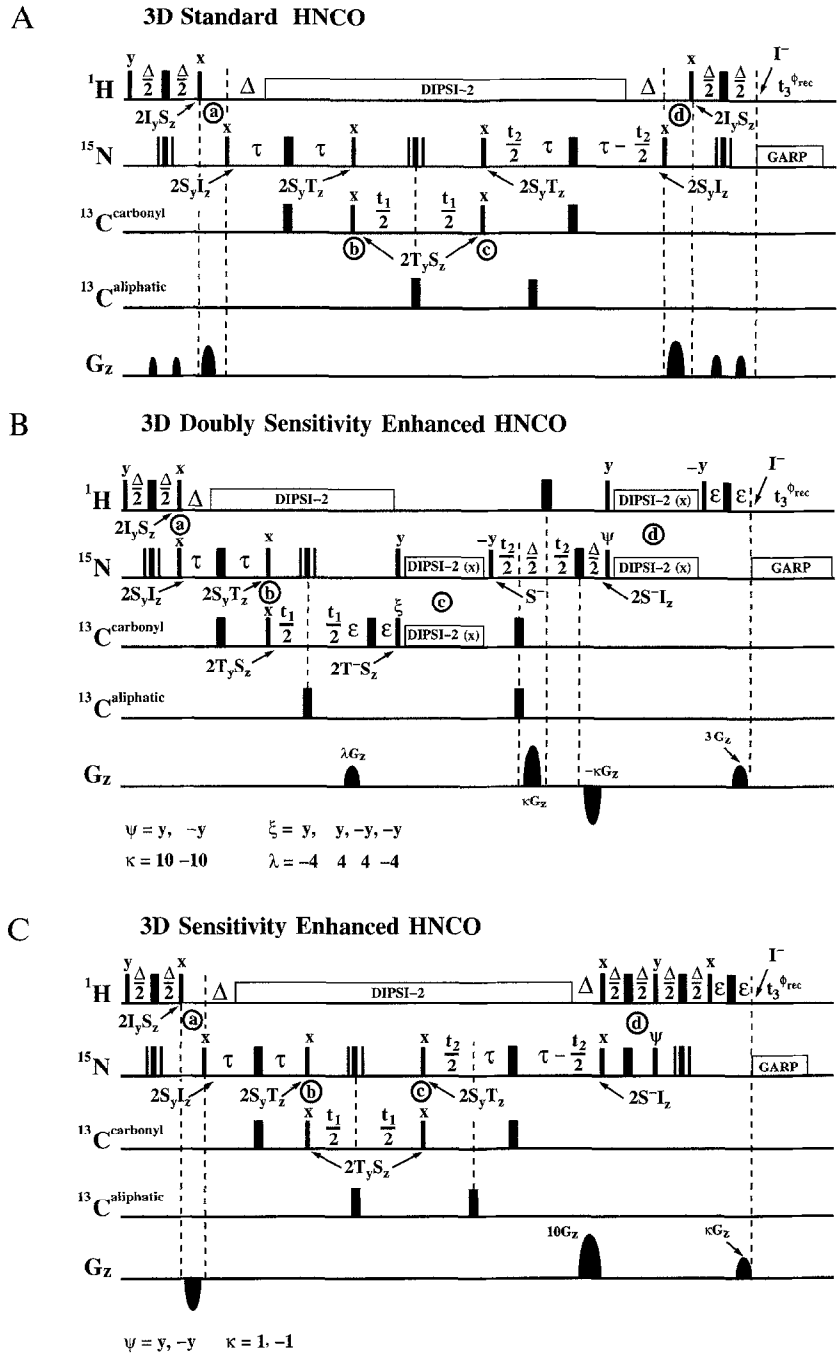

Fig. 4. (A) Conventional HNCO experiment with transfer of Cartesian operators from C' to N and from N to H. (B) Double sensitivity-enhanced HNCO. The antiphase $C' \rightarrow N$ transfer $2S_zT^- \rightarrow S^-$ is accomplished with a planar heteronuclear TOCSY; the dephasing of nitrogen in-phase magnetization $S^- \rightarrow 2S^-I_z$, followed by an $N \rightarrow H$ COS-CT ($2S^-I_z \rightarrow I^-$) via planar TOCSY, can be considered as in-phase COS-CT $S^- \rightarrow I^-$. This COS-CT can be substituted by the sequence shown in Fig. 1E, with a slight increase in sensitivity. (C) Sensitivity-enhanced HNCO with an anti-phase COS-CT only for the anti-phase $N \rightarrow H$ transfer: $2S^-I_z \rightarrow I^-$. This sequence is much shorter than the sequence in (B) and therefore does not suffer from the decay of transverse magnetization (cf. Eq. 6) as in sequence B.

shift evolution, employing COS-CT in combination with a heteronuclear gradient echo, is identical to a conventional H(N)CO experiment without gradients. The experimental performance can be judged from Fig. 5. Since the sequence of Fig. 4C with ^{15}N chemical shift evolution achieves almost the full sensitivity enhancement of $\sqrt{2}$, the S/N of the relayed H(N)CO experiment with gradient and COS-CT is comparable to the S/N obtained from a conventional pulse sequence without gradients.

The experiments were recorded on a 2 mM sample of the protein rhodniin (103 residues), dissolved in H_2O/D_2O (10 : 1) in a Shigemi tube. Analysis of 91 signals gives a relative S/N ratio of $1 : 1.22 \pm 0.18 : 1.31 \pm 0.11$ for the conventional HNCO, the doubly enhanced HNCO

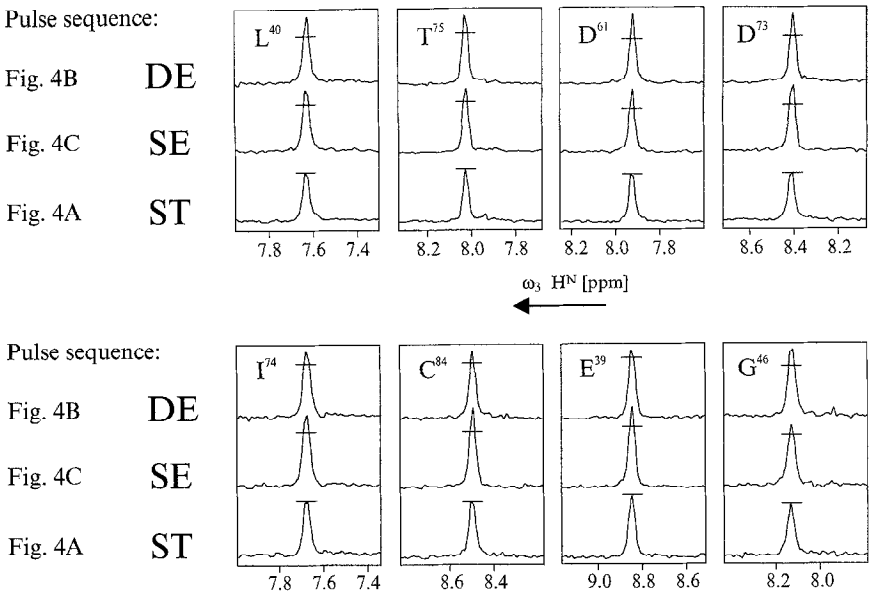

Fig. 5. Sensitivity enhancement in 3D HNCO. Shown are ω_3 traces from the 3D HNCO experiment through representative H^N resonances of rhodniin: Leu[40], Thr[75], Asp[61], Asp[73], Ile[74], Cys[84], Glu[39] and Gly[46], obtained with the conventional (ST) HNCO of Fig. 4A (bottom trace), the singly enhanced (SE) HNCO of Fig. 4C (middle trace) and the doubly enhanced (DE) HNCO of Fig. 4B (top trace). The bars indicate the signal height in the conventional experiment. On average, the SE HNCO and the DE HNCO have 1.31 and 1.22 of the intensity of the ST HNCO, respectively.

and the singly enhanced HNCO, respectively. Thus, the sequence depicted in Fig. 4C achieves almost the predicted enhancement of a factor of $\sqrt{2}$, whereas the signal is attenuated due to relaxation in the sequence of Fig. 4B, which employs two COS-CTs from $C' \rightarrow N$ and $N \rightarrow H^N$. This loss of enhancement can be understood if one considers that the sequence in Fig. 4B is longer than the sequence in Fig. 4C by $1/(2J_{C',N}) + 1/(2J_{N,H^N}) \sim 38$ ms. Compared to the sequence in Fig. 4C, the signal loss due to relaxation during 38 ms with $T_2 \sim 100$ ms is 0.68, which is not compensated by the additional factor $\sqrt{2}$ due to application of COS-CT. Therefore, in this example COS-CT should only be used for the $N \rightarrow H$ transfer, in which the coupling constant is much larger than the line width.

HCCH-TOCSY

As a second example, we present an application of concatenation of multiple COS-CTs in 3D H(C)CH-TOCSY experiments. A standard (ST) H(C)CH-TOCSY with presaturation of the water resonance (Fig. 6A), the sensitivity-enhanced gradient version (SE) employing COS-CT for the final transfer from C to H between t_2 and t_3 (Fig. 6B), and an H(C)CH-TOCSY employing COS-CT throughout the pulse sequence (DE) (Figs. 6C and D) are compared.

The sequence in Fig. 6A employs heteronuclear Hartmann-Hahn transfer from proton to carbon during τ_1, while homonuclear TOCSY between carbons is active during τ_2. Only one Cartesian component is transferred in the heteronuclear Hartmann-Hahn mixing ($F_x \rightarrow S_{ax}$). Water suppression is achieved by presaturation and the gradient during delay ε, when the water magnetization is transverse whereas the magnetization of protons bound to ^{13}C is longitudinal. The suppression of the water resonance is not satisfactory, as can be seen in the spectrum of Fig. 7A.

In the sequence in Fig. 6B, an in-phase COS-CT according to Fig. 1D is used for the final $C \rightarrow H$ transfer. The water is completely suppressed by the heteronuclear gradient echo (not shown, but compare to Fig. 7B). Equal sensitivity as in the non-gradient experiment is expected for CH_2 and CH_3 groups, whereas a maximum sensitivity enhancement of 1.2 is expected for CH groups.

In the sequence in Fig. 6C, the $H \rightarrow C \rightarrow C$ transfer is accomplished by generation of the initial operator $2F^-S_{az}$ by defocussing during $\Delta = 1/(2\,^1J(C,H))$ and then by a combination of heteronuclear planar TOCSY and isotropic mixing applied to the carbons for the transfer $2F^-S_{az} \rightarrow S_a^- \rightarrow S_b^-$. For a homonuclear spin system, the DIPSI-2 sequence (Shaka et al., 1988) generates an isotropic coupling Hamiltonian: $S_{ax}S_{bx} + S_{ay}S_{by} + S_{az}S_{bz}$ (S_a and S_b denote two J-coupled carbon spins). This Hamiltonian is invariant under rotation by the two 90° (^{13}C) pulses. The effective Hamiltonian crafted from the heteronuclear coupling $2\pi JF_zS_z$ is given by $\pi J(F_xS_x + F_yS_y)$, which is known to transfer antiphase magnetization of the type $2F^-S_z$ to S^- (Schleucher et al., 1994). Thus, the heteronuclear $H \rightarrow C$ and the homonuclear $C \rightarrow C$ transfer are both coherence order selective. Defocussing of the heteronuclear coupling has to be done during Δ, in order to obtain the essential antiphase operator $2F^-S_{az}$ at the end of the first evolution time.

The homonuclear isotropic C,C-TOCSY can also be combined with sequences accomplishing in-phase COS

transfer $F^- \rightarrow S^-$, like the sequence in Fig. 1D (pulse sequence in Fig. 6D) or the isotropic heteronuclear Hartmann-Hahn mixing (pulse sequence in Fig. 6E). Since the available heteronuclear isotropic mixing sequences (Weitekamp et al., 1982,1983; Caravatti et al., 1983) do not cover a sufficient broadband frequency range for a feasible rf power, optimized heteronuclear isotropic mixing schemes are currently under development.

The excellent water suppression in the spectra with

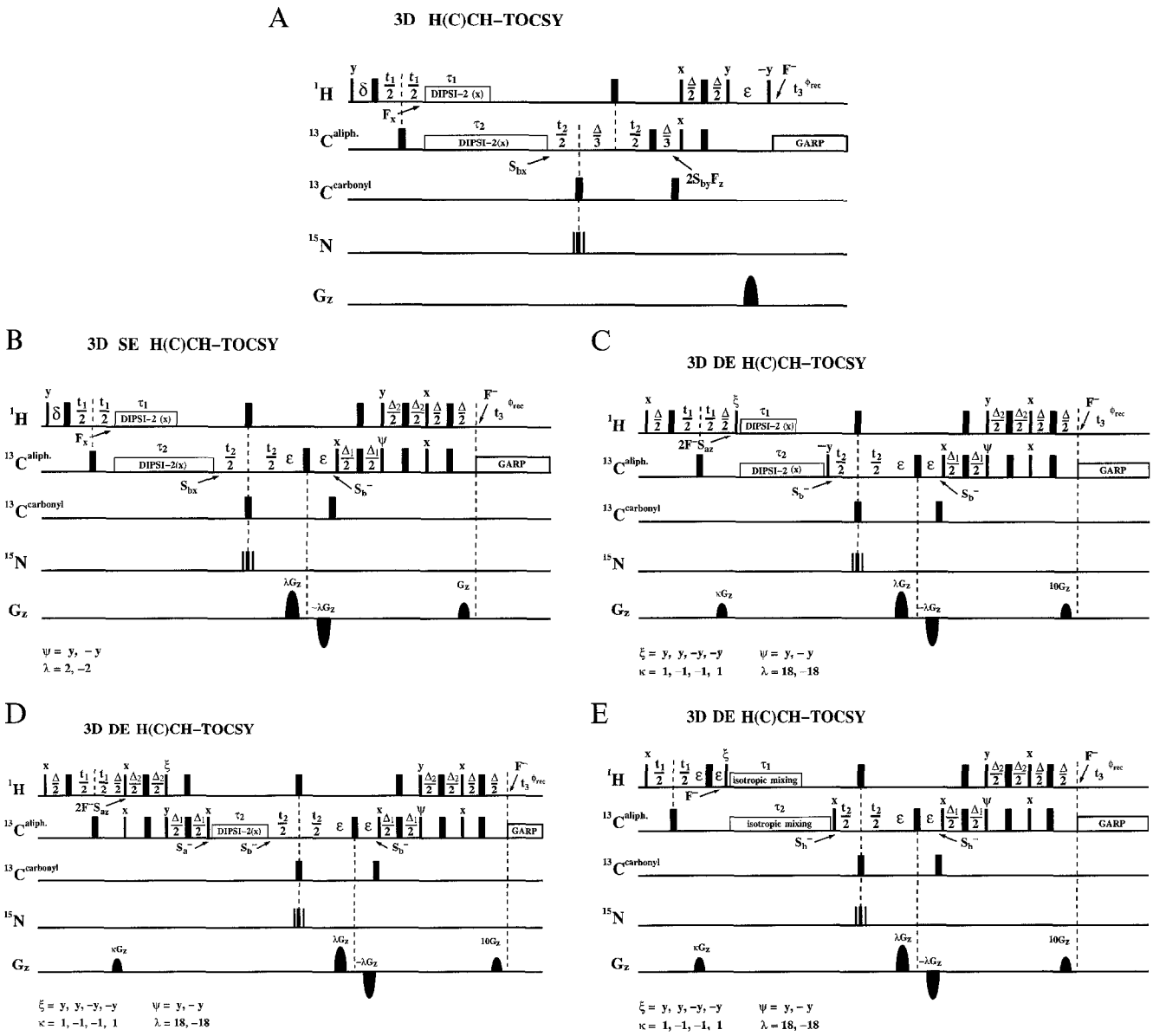

Fig. 6. (A) 3D H(C)CH-TOCSY with a heteronuclear Hartmann-Hahn transfer, combined with homonuclear C,C-TOCSY and a conventional INEPT transfer from carbon to proton, achieving the transfer $F_x \rightarrow S_{ax} \rightarrow S_{bx} \rightarrow F^-$, with $F_x = \Sigma_i(I_{ix})$. Product operators describe the fate of the magnetization through the sequence. Water suppression is achieved by presaturation and a homospoil pulse during ε. The delay δ should be equal to the 180°(^{13}C) pulse duration to avoid chemical shift evolution for the first t_1 increment, so that $t_1(0) = 0$. (B) 3D sensitivity-enhanced H(C)CH-TOCSY. The C → H transfer at the end of the sequence is replaced by an in-phase COS-CT according to Fig. 1D. An enhancement factor up to 1.2 is expected. Excellent water suppression is achieved, due to the heteronuclear gradient echo (compare to Fig. 7B). The delay δ should be equal to the 180°(^{13}C) pulse duration to avoid chemical shift evolution for the first t_1 increment. (C) 3D doubly enhanced HCCH-TOCSY. The C → H transfer is the same as in Fig. 4B. The H(C)C transfer, however, is accomplished here by creation of antiphase coherence $2S_{az}F^-$ which is transferred to S_b^- by planar heteronuclear TOCSY and simultaneous isotropic mixing of the S spins. Therefore, all coherence transfers are coherence order selective. A maximum enhancement of a factor 2 is expected. (D) 3D doubly enhanced HCCH-TOCSY. The C → H transfer is the same as in Fig. 4B. The H(C)C transfer, however, is accomplished using the sequence of Fig. 1D for the transfer $F^- \rightarrow S_a^-$, in conjunction with homonuclear C,C-TOCSY for the transfer $S_a^- \rightarrow S_b^-$. Like in sequence (C), all transfer steps are coherence order selective, thus a maximum enhancement factor of 2 is expected. (E) 3D doubly enhanced H(C)CH-TOCSY experiment. The C → H transfer is the same as in Fig. 4B. The H(C)C transfer, however, is accomplished using isotropic mixing for the heteronuclear transfer in combination with isotropic mixing for the homonuclear C,C transfer. Again, both steps are coherence order selective. Since the available heteronuclear isotropic mixing sequences (Weitekamp et al., 1982,1983; Caravatti et al., 1983) are not sufficiently broadband, this pulse scheme was not tested experimentally.

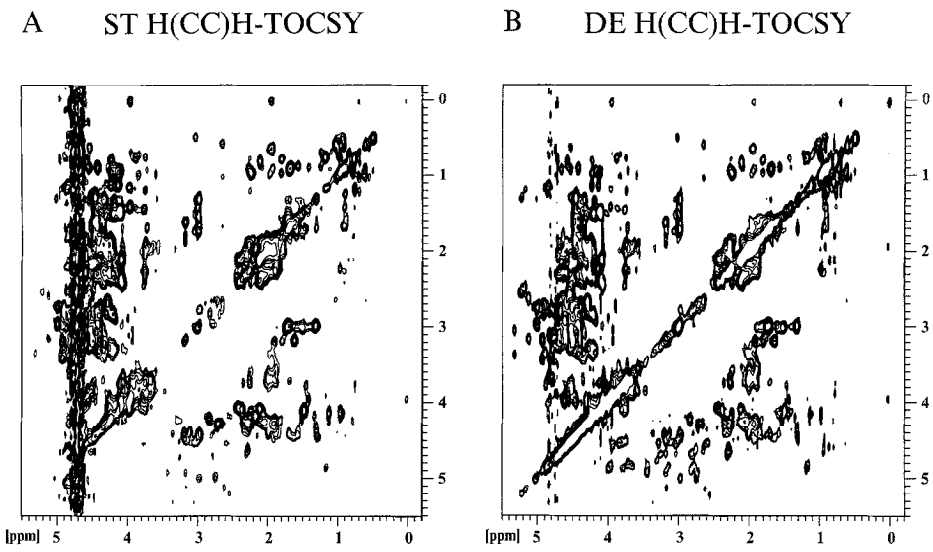

Fig. 7. First 2D plane ($t_2 = 0$) through the H(C)CH-TOCSY spectra obtained by the sequences in Figs. 6A and C for a 2 mM $^{13}C/^{15}N$-labeled sample of rhodniin in $H_2O : D_2O$ (10 : 1). (A) The spectrum obtained with the sequence of Fig. 6A shows a strong water ridge that makes the cross peaks around 4.7 ppm not interpretable. (B) The doubly enhanced H(C)CH-TOCSY spectrum obtained from the pulse sequence in Fig. 6C, which employed a slightly less sensitive C → H back-transfer (see text), shows almost no residual water resonance.

heteronuclear gradient echo (Fig. 7B) obtained with the sequence in Fig. 6C can be estimated from the H,H correlation in the first 2D spectrum ($t_2 = 0$). By contrast, the region under the water resonance in the 2D slice (Fig. 7A) obtained from the conventional presaturation experiment (Fig. 6A) cannot be interpreted. The spectra were recorded on the sample of rhodniin.

In order to find the optimal mixing times for the $^1H \rightarrow {}^{13}C \rightarrow {}^{13}C$ transfers, numerical simulations (Fig. 8) were performed of the $H \rightarrow C \rightarrow C$ transfer that is achieved by a heteronuclear transfer sequence during τ_{HC}, in combination with the generation of an isotropic J-coupling Hamiltonian for the C,C transfer during τ_2. For the heteronuclear coherence transfer, the transfer amplitudes of three implementations are compared: (i) conventional heteronuclear Hartmann-Hahn mixing ($\mathbf{H}_m = \pi J (I_y S_y + I_z S_z)$), used in Figs. 6A and B during τ_1 (Fig. 8A) for the in-phase transfer $F_x \rightarrow S_{ax}$; (ii) defocussing of in-phase magnetization F^- during $\Delta = 1/(2J_{IS})$, followed by COS-CT $2F^-S_{az} \rightarrow S_a^-$ using a planar coupling Hamiltonian ($\mathbf{H}_{xy} = \pi J (I_x S_x + I_y S_y)$; Fig. 6C) during τ_1 (Fig. 8B), which effectively accomplishes in-phase COS-CT $F^- \rightarrow S_a^-$; and (iii) in-phase COS-CT $F^- \rightarrow S_a^-$, either by a pulse sequence (Figs. 6D and 8C,D) or by an isotropic heteronuclear J-coupling Hamiltonian (Figs. 6E and 8E).

The $H \rightarrow C \rightarrow C$ transfer efficiencies are determined for different C-H multiplicities in different spin systems, namely for $H^{13}C$-^{13}C, ^{13}C-$H_2{}^{13}C$-^{13}C and $H_3{}^{13}C$-^{13}C spin systems, which are the most frequently encountered coupling topologies for HC, H_2C and H_3C moieties in proteins. Weak coupling is assumed between heteronuclear spins, and strong coupling is assumed between homonuclear spins only during Hartmann-Hahn mixing.

For all sequences except for that in Fig. 6D, two delays are varied. For the sequence in Fig. 6D, with the three variable delays Δ_1, Δ_2 and τ_2, optimal Δ_1, τ_2 slices are given for each multiplicity. In addition, a slice through $\Delta_2^{opt} = 2.2$ ms is shown that yields optimal sensitivity for all multiplicities. In all slices the optimal values for each multiplicity are given separately in the figure and are indicated by an asterisk. The values that are optimal as a compromise for all multiplicities simultaneously are indicated as diamonds, and the experimental ones are given as filled circles. The results of the simulations are summarized in Table 1, where the *maximum transfer* corresponds to the maximum for each multiplicity and the *multiplicity-averaged optimum transfer* corresponds to delay settings which optimize the transfer amplitudes for CH, CH_2 and CH_3 simultaneously. These delays are found by minimizing the expression $\Sigma_{i=1}^{n} W_i (I_i^{max} - I_i)^2$, where W_i is the weight and I_i^{max} and I_i are the maximum and the actual transfer amplitudes for each multiplicity. The weight factors were 2, 2 and 1, for CH, CH_2 and CH_3, respectively, because the sensitivity of CH and CH_2 groups is more critical than that of CH_3 groups. In addition, the transfer times for the $H \rightarrow C$ (τ_{HC}) and the $C \rightarrow C$ (τ_2) coherence transfer, as well as the total time for the coherence transfer $H \rightarrow C \rightarrow C$ (τ_{CT}) are given in Table 1 for the multiplicity-averaged delay settings.

From the theoretical simulations, it turns out that the sequence of Figs. 6E and 8E with isotropic heteronuclear and isotropic homonuclear mixing has the best performance. However, no broadband heteronuclear isotropic sequences have been developed to date and therefore this sequence could not be tested experimentally.

Experimental results are shown in Figs. 7 and 9. To

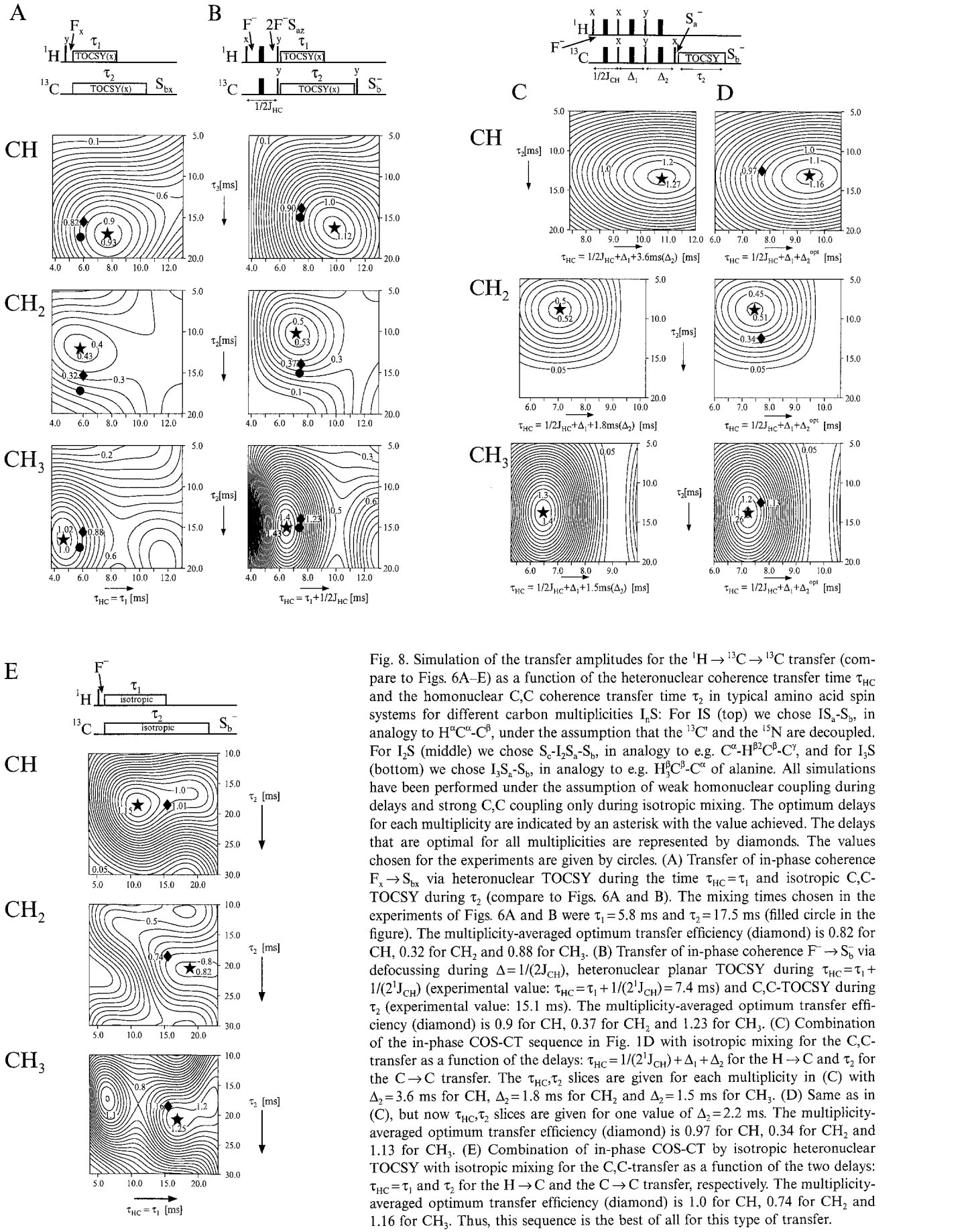

Fig. 8. Simulation of the transfer amplitudes for the $^1H \rightarrow {}^{13}C \rightarrow {}^{13}C$ transfer (compare to Figs. 6A–E) as a function of the heteronuclear coherence transfer time τ_{HC} and the homonuclear C,C coherence transfer time τ_2 in typical amino acid spin systems for different carbon multiplicities I_nS: For IS (top) we chose IS_a-S_b, in analogy to $H^{\alpha}C^{\alpha}$-C^{β}, under the assumption that the $^{13}C'$ and the ^{15}N are decoupled. For I_2S (middle) we chose S_c-I_2S_a-S_b, in analogy to e.g. C^{α}-$H^{\beta 2}C^{\beta}$-C^{γ}, and for I_3S (bottom) we chose I_3S_a-S_b, in analogy to e.g. $H^{\beta}_3C^{\beta}$-C^{α} of alanine. All simulations have been performed under the assumption of weak homonuclear coupling during delays and strong C,C coupling only during isotropic mixing. The optimum delays for each multiplicity are indicated by an asterisk with the value achieved. The delays that are optimal for all multiplicities are represented by diamonds. The values chosen for the experiments are given by circles. (A) Transfer of in-phase coherence $F_x \rightarrow S_{bx}$ via heteronuclear TOCSY during the time $\tau_{HC} = \tau_1$ and isotropic C,C-TOCSY during τ_2 (compare to Figs. 6A and B). The mixing times chosen in the experiments of Figs. 6A and B were $\tau_1 = 5.8$ ms and $\tau_2 = 17.5$ ms (filled circle in the figure). The multiplicity-averaged optimum transfer efficiency (diamond) is 0.82 for CH, 0.32 for CH_2 and 0.88 for CH_3. (B) Transfer of in-phase coherence $F^- \rightarrow S_b^-$ via defocussing during $\Delta = 1/(2J_{CH})$, heteronuclear planar TOCSY during $\tau_{HC} = \tau_1 + 1/(2^1J_{CH})$ (experimental value: $\tau_{HC} = \tau_1 + 1/(2^1J_{CH}) = 7.4$ ms) and C,C-TOCSY during τ_2 (experimental value: 15.1 ms). The multiplicity-averaged optimum transfer efficiency (diamond) is 0.9 for CH, 0.37 for CH_2 and 1.23 for CH_3. (C) Combination of the in-phase COS-CT sequence in Fig. 1D with isotropic mixing for the C,C-transfer as a function of the delays: $\tau_{HC} = 1/(2^1J_{CH}) + \Delta_1 + \Delta_2$ for the $H \rightarrow C$ and τ_2 for the $C \rightarrow C$ transfer. The τ_{HC},τ_2 slices are given for each multiplicity in (C) with $\Delta_2 = 3.6$ ms for CH, $\Delta_2 = 1.8$ ms for CH_2 and $\Delta_2 = 1.5$ ms for CH_3. (D) Same as in (C), but now τ_{HC},τ_2 slices are given for one value of $\Delta_2 = 2.2$ ms. The multiplicity-averaged optimum transfer efficiency (diamond) is 0.97 for CH, 0.34 for CH_2 and 1.13 for CH_3. (E) Combination of in-phase COS-CT by isotropic heteronuclear TOCSY with isotropic mixing for the C,C-transfer as a function of the two delays: $\tau_{HC} = \tau_1$ and τ_2 for the $H \rightarrow C$ and the $C \rightarrow C$ transfer, respectively. The multiplicity-averaged optimum transfer efficiency (diamond) is 1.0 for CH, 0.74 for CH_2 and 1.16 for CH_3. Thus, this sequence is the best of all for this type of transfer.

TABLE 1
MAXIMUM AND OPTIMUM TRANSFER AMPLITUDES FOR IN-PHASE COHERENCE TRANSFER $^1H \rightarrow {}^{13}C \rightarrow {}^{13}C$

Experiment		Maximum transfer amplitudes			Optimum transfer amplitudes					
		CH	CH_2	CH_3	CH	CH_2	CH_3	τ_{HC} (ms)	τ_2 (ms)	τ_{CT} (ms)
Conventional CT	Fig. 8A	0.93	0.43	1.02	0.82	0.32	0.88	$\tau_1 = 6.0$	15.5	$\tau_2 = 15.5$
COS-CT	Fig. 8B	1.12	0.53	1.43	0.90	0.37	1.23	$1/(2J_{CH}) + \tau_1 = 7.5$	14.0	$1/(2J_{CH}) + \tau_2 = 17.8$
In-phase COS-CT	Fig. 8C	1.27	0.52	1.40						
	Fig. 8D				0.97	0.34	1.13	$\Delta_1 + \Delta_2 + 1/(2J_{CH}) = 7.7$	12.5	$\Delta_1 + \Delta_2 + 1/(2J_{CH}) + \tau_2 = 20.2$
Isotropic mixing	Fig. 8E	1.15	0.82	1.25	1.01	0.74	1.16	$\tau_1 = 15.5$	18.5	$\tau_2 = 18.5$

obtain optimum sensitivity for CH, CH_2 and CH_3 multiplicities at the same time, heteronuclear TOCSY mixing times of $\tau_1 = 5.8$ ms and 3.6 ms were chosen for the conventional (Figs. 6A,B) and the COS-CT experiments (Fig. 6C), respectively. Since the conventional and the COS-CT heteronuclear TOCSY sequences rely on different transfer mechanisms, the distribution of the $H \rightarrow C \rightarrow C$ transfer amplitudes across the spin system cannot be expected to be identical. This can be appreciated also from Fig. 8. Therefore, the signal-to-noise ratio of the total spin system has to be compared for the different spectra.

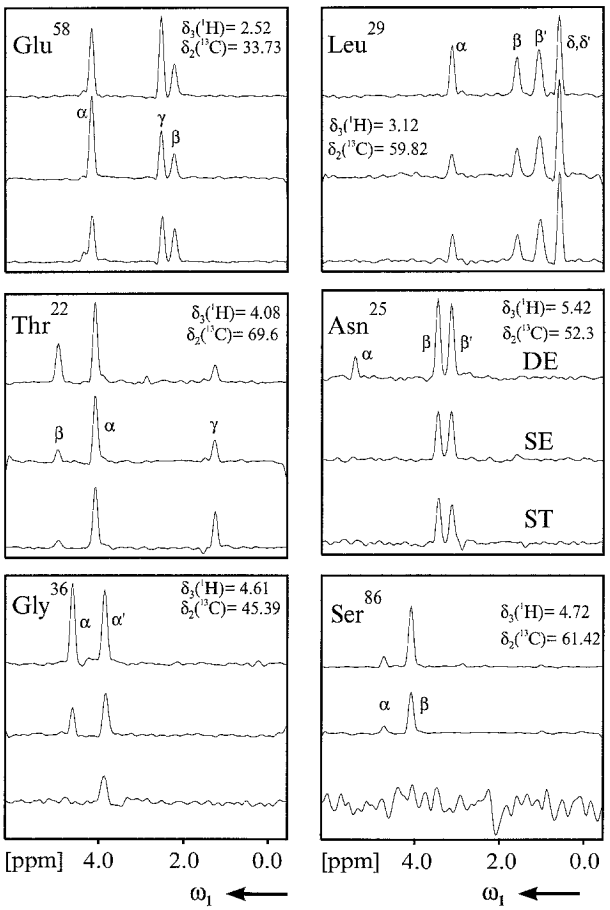

Fig. 9. Slices through the 3D H(C)CH-TOCSY spectra obtained from the sequences in Figs. 6A (ST), 6B (SE) and 6C (DE) for Glu^{58}, Thr^{22}, Gly^{36}, Leu^{29}, Asn^{25} and Ser^{86}. The $C \rightarrow H$ transfer employed for the SE and DE spectra was slightly less sensitive than the one given in Figs. 6B and C (see text). The traces through the Ser^{86} H^{α} show the quality of the water suppression in the spectra with heteronuclear gradient echoes. Overall, the expected sensitivity enhancement is visible. However, as explained in more detail in the text, the enhancement is not achieved uniformly for all resonances, because the Hamiltonians in the different implementations of the pulse sequence cannot be matched.

Representative ω_1 traces for the three 3D experiments are given in Fig. 9, clearly showing that the sensitivity in the three experiments increases from the standard (ST) to the singly enhanced (SE) and the doubly enhanced (DE) spectra. An analysis of 28 spin systems results in the following average relative sensitivities: ST / SE / DE: $1 / 1.11 \pm 0.16 / 1.34 \pm 0.36$. The rather large standard deviation for the sensitivity enhancement of the DE spectrum is a result of the different multiplicity composition of the different spin systems. Furthermore, not each individual peak in the DE spectrum shows enhancement over the ST spectrum, since the use of different effective Hamiltonians cannot be compensated for by a single set of mixing times. It should be noted that a slightly less sensitive sequence than that given in Figs. 6B and C was used for the $C \rightarrow H$ back-transfer in the SE and DE experiments (using a delay of $0.3/{}^1J(H,C)$ for the transfer $S^- \rightarrow 2S^-F_z$, followed by the COS-INEPT sequence given in Fig. 1A). Thus, employing the pulse sequences given in Figs. 6B and C, the sensitivity enhancement could be further improved compared to the ST sequence. The optimum solvent suppression in the experiments which employ a heteronuclear gradient echo for the $C \rightarrow H$ back-transfer can be seen in the two lower traces, where detection of ^1H resonances close to the H_2O signal is almost impossible in the presaturation experiment.

Conclusions

We have shown that **C**oherence **O**rder **S**elective **C**oherence **T**ransfers (COS-CTs), employing heteronuclear gradient echoes, can be combined in multidimensional NMR experiments and lead to improved signal-to-noise ratio and excellent water suppression. Sequences have been proposed and experimentally tested that make use of recently developed pulse sequence elements, e.g. COS-INEPT and planar TOCSY for antiphase to in-phase

transfers $2F^-S_z \leftrightarrow S^-$, or in-phase COS-CT for in-phase transfers $F^- \leftrightarrow S^-$, and the well-known homonuclear and heteronuclear isotropic TOCSY mixing sequences for homo- and heteronuclear in-phase transfer. We have shown that, depending on the size of the relevant J-coupling and relaxation times, full enhancement cannot always be achieved due to relaxation losses. However, even in these cases it is advantageous to use COS-CT for selected coherence transfer steps in combination with a heteronuclear gradient echo, as this yields spectra of S/N comparable to conventional experiments, but with a far superior water suppression.

Acknowledgements

This work was supported by the Fonds der Chemischen Industrie and the DFG under Gr. 1211/6-1. M.G.S. and J.S. were supported by the DFG via the Graduiertenkolleg 'Chemische und Biologische Synthese von Wirkstoffen' (Gk Eg 53/3-3). M.G.S. is grateful for a Schrödinger scholarship of the Austrian 'Fonds zur Förderung der wissenschaftlichen Forschung': J0692-CHE. We are grateful to Dr. U. Weydemann (Rhein Biotech, Düsseldorf) who prepared the sample of rhodniin. We thank Dr. T. Keller, Dr. W. Bermel and Dr. R. Kerssebaum (Bruker Karlsruhe) for continuous support.

References

Braunschweiler, L. and Ernst, R.R. (1983) *J. Magn. Reson.*, **53**, 521–528.

Caravatti, P., Braunschweiler, L. and Ernst, R.R. (1983) *Chem. Phys. Lett.*, **100**, 305–310.

Cavanagh, J. and Rance, M. (1990) *J. Magn. Reson.*, **88**, 72–85.

Cavanagh, J. and Rance, M. (1993) *Annu. Rep. NMR Spectrosc.*, **27**, 1–58.

Davis, A.L., Keeler, J., Laue, E.D. and Moskau, D. (1992) *J. Magn. Reson.*, **98**, 207–216.

Hurd, R.E. and John, B.K. (1991) *J. Magn. Reson.*, **91**, 648–653.

Kay, L.E., Keifer, P. and Saarinen, T. (1992) *J. Am. Chem. Soc.*, **114**, 10663–10665.

Levitt, M.H. (1992a) In *Pulsed Magnetic Resonance: NMR, ESR, and Optics. A Recognition of E.L. Hahn* (Ed., Bagguley, D.M.S.) Clarendon Press, Oxford, pp. 184–201.

Levitt, M.H. (1992b) *J. Magn. Reson.*, **99**, 1–17.

Maudsley, A.A., Wokaun, A. and Ernst, R.R. (1978) *Chem. Phys. Lett.*, **55**, 9–14.

Muhandiram, D.R., Xu, G.Y. and Kay, L.E. (1993) *J. Biomol. NMR*, **3**, 463–470.

Muhandiram, D.R. and Kay, L.E. (1994) *J. Magn. Reson. Ser. B*, **103**, 203–216.

Nielsen, N.C. and Sørensen, O.W. (1992) *J. Magn. Reson.*, **99**, 449–465.

Palmer III, A.G., Cavanagh, J., Wright, P.E. and Rance, M. (1991) *J. Magn. Reson.*, **93**, 151–170.

Redfield, A.G. (1991) *J. Magn. Reson.*, **92**, 642–644.

Sattler, M., Schmidt, P., Schleucher, J., Schedletzky, O., Glaser, S.J. and Griesinger, C. (1995) *J. Magn. Reson. Ser. B*, in press.

Schleucher, J., Sattler, M. and Griesinger, C. (1993a) *Angew. Chem.*, **105**, 1518–1521.

Schleucher, J., Sattler, M. and Griesinger, C. (1993b) *Angew. Chem., Int. Ed. Engl.*, **32**, 1489–1491.

Schleucher, J., Schwendinger, M.G., Sattler, M., Schmidt, P., Glaser, S.J., Sørensen, O.W. and Griesinger, C. (1994) *J. Biomol. NMR*, **4**, 301–306.

Schulte-Herbrüggen, T., Madi, Z.L., Sørensen, O.W. and Ernst, R.R. (1991) *Mol. Phys.*, **72**, 847–874.

Shaka, A.J., Lee, C.J. and Pines, A. (1988) *J. Magn. Reson.*, **77**, 274–293.

Sørensen, O.W. (1989) *Prog. NMR Spectrosc.*, **21**, 503–570.

Sørensen, O.W. (1990) *J. Magn. Reson.*, **86**, 435–440.

Sørensen, O.W. (1991) *J. Magn. Reson.*, **93**, 648–652.

Stoustrup, J., Schedletzky, O., Glaser, S.J., Griesinger, C., Nielsen, N.C. and Sørensen, O.W. (1995) *Phys. Rev. Lett.*, **74**, 2921–2924.

Vuister, G.W. and Bax, A. (1994) Poster WP 142, 35th ENC, April 10–15, Asilomar, CA.

Weitekamp, D.P., Garbow, J.R. and Pines, A. (1982) *J. Chem. Phys.*, **77**, 2870–2883.

Weitekamp, D.P., Garbow, J.R. and Pines, A. (1983) *J. Chem. Phys.*, **80**, 1372.